Z. Angew. Math. Mech., vol. 79, pp. S199–S202, 1999.

FOREST, S.; PILVIN, P.

Modelling Finite Deformation of Polycrystals Using Local Objective Frames

The formulation of constitutive models at finite strain using local objective frames is applied to solids with microstructure. Priviledged space frames are introduced at both the material level and the microstructure level. For single crystals, the method leads to a model almost equivalent to Mandel's theory. For polycrystals, an explicit concentration rule written in the corotational frame is proposed. Simulations of texture evolutions are then presented.

1. Introduction

The use of local objective frames, recommended for instance in [5,7], has proved to be an efficient method to develop constitutive models at finite strain, that automatically fulfill the material frame indifference requirement. A local space frame E_X is defined for each material point X by the rotation field $\underset{\sim}{\mathbf{Q}}_X(t)$ with respect to the current space frame E. It is said to be objective if, for any space frame E' related to E by the rotation $\underset{\sim}{\mathbf{Q}}'(t)$, the rotation field linking E' to E_X is $\underset{\sim}{\mathbf{Q}}'_X = \underset{\sim}{\mathbf{Q}}_X \underset{\sim}{\mathbf{Q}}^T, \forall t$. Local objective frames can also be used to extend, in a straightforward manner, constitutive equations that have been developed at small strains, to the finite strain framework, as proposed in [9]. The choice of the local objective reference frame in which the constitutive equations are written, then becomes a major issue in the modelling. Dogui and Sidoroff [5] have weighted the pros and the cons for the use of the corotational frame, which is associated with the skew-symmetric part of the velocity gradient $\underset{\sim}{\mathbf{L}}$, and of the "eigenrotational" frame which involves the rotation in the polar decomposition of the deformation gradient $\underset{\sim}{\mathbf{F}}$. As for him, Rougée [12] resorts to an intrinsic description of material behaviour, and he shows that a canonical material derivative exists if one considers the non-Euclidean structure of the manifold $\mathbf{M}$ of all local metric states. The Euclidean counterpart of this covariant derivative turns out to be the Jaumann rate which is related to the corotational frame. This endows the corotational frame with a strong geometrical meaning.

When one aims at taking some features of material microstructure into account, one may think that the corotational or the "eigenrotational" frames can be of no use because they do not incorporate any available physical information. In contrast, we propose here to introduce local objective frames at two levels into the modelling. The first one, called material level, is of purely geometrical nature: we choose an observer to follow the rotation of material fibers. This can be done only in an approximate manner [7], and, for that purpose, we retain the corotational frame. On the other hand, at the microstructural level, we will assume that a frame can be attached to each element of microstructure retained in the modelling. Its rotation will then be measured with respect to the first observer. By using the corotational frame, we get rid of material rotations that do not intervene in the material behaviour. This gives furthermore a privileged point of view from which the evolution of the microstructure (grain rotation in a polycrystal for instance) can be observed. We lay the stress on the fact that the corotational frame best follows, at a given time and in average, strain gauges that are stuck on a specimen for testing. Consequently, when such measurements are the only way to have direct access to material behaviour, an efficient and reliable inductive method for developing constitutive equations, consists in infering them directly in the corotational frame.

We apply successively this program to f.c.c. single crystals and polycrystals. In the following, $Y, \underline{\mathbf{Y}}, \underset{\sim}{\mathbf{Y}}$ and $\underset{\approx}{\mathbf{Y}}$ respectively denote a scalar, a vector, a second-rank and a four-rank tensor.

2. Finite deformation of single crystals

Let $E, E^c, E^\sharp$ respectively be the current space frame, the corotational space frame and a lattice space frame. Variable y will be denoted y, ${}^c y$, ${}^\sharp y$, when considered with respect to $E, E^c, E^\sharp$. Rotation ${}^c\underset{\sim}{\mathbf{Q}}$ links E^c to E and rotation ${}^\sharp\underset{\sim}{\mathbf{Q}}$, $E^\sharp$ to E^c. The corotational frame is defined by

$$ {}^c\dot{\underset{\sim}{\mathbf{Q}}}\ {}^c\underset{\sim}{\mathbf{Q}}^T = {}^\}\underset{\sim}{\mathbf{L}}^\{ \quad \text{and} \quad {}^c\underset{\sim}{\mathbf{Q}}(t_0) = \underset{\sim}{\mathbf{1}}, \tag{1} $$

where the inverted brackets denote the skew-symmetric part of the expression. We adopt an additive partition of the strain rate in the corotational frame into its elastic and viscoplastic parts

$$ {}^c\underset{\sim}{\mathbf{D}} \;=\; {}^c\underset{\sim}{\mathbf{Q}}^T \,\{\underset{\sim}{\mathbf{L}}\}\; {}^c\underset{\sim}{\mathbf{Q}} \;=\; \dot{\underset{\sim}{\mathbf{e}}}^e \;+\; \dot{\underset{\sim}{\mathbf{e}}}^p, \tag{2} $$

where the brackets denote the symmetric part. The elastic law reads

$$ \underset{\sim}{\mathbf{S}} \;=\; \underset{\sim}{\mathbf{C}}\;\underset{\sim}{\mathbf{e}}^e, \quad \text{with} \quad \underset{\sim}{\mathbf{S}} \;=\; (\mathrm{Det}\;\underset{\sim}{\mathbf{F}})\; {}^c\underset{\sim}{\mathbf{Q}}^T\; \underset{\sim}{\mathbf{T}}\; {}^c\underset{\sim}{\mathbf{Q}}, \tag{3} $$

where $\underset{\sim}{\mathbf{T}}$ is the Cauchy stress tensor. In single crystals, viscoplastic deformation proceeds through collective glide of dislocations according to particular slip systems

$$ \dot{\underset{\sim}{\mathbf{e}}}^p \;=\; \sum_{s\in S} \dot\gamma^s \;\{\, {}^c\underline{\mathbf{m}}^s \otimes {}^c\underline{\mathbf{z}}^s\}. \tag{4} $$

$\underline{\mathbf{m}}^s$ and $\underline{\mathbf{z}}^s$ respectively are the slip direction and the normal to the slip plane for slip system s. γ^s is the associated slip amount. Evolution equations for these variables are given in the next section. The yield criterion is based on Schmid law. The second local frame is attached to the lattice and its rotation is given by

$$ {}^\sharp\dot{\underset{\sim}{\mathbf{Q}}}\; {}^\sharp\underset{\sim}{\mathbf{Q}}^T \;=\; -\sum_{s\in S} \dot\gamma^s \;\}\, {}^c\underline{\mathbf{m}}^s \otimes {}^c\underline{\mathbf{z}}^s\{ \quad \text{and} \quad {}^\sharp\underset{\sim}{\mathbf{Q}}(t_0) \;=\; \underset{\sim}{\mathbf{1}}. \tag{5} $$

Crystallographic directions are known in the lattice frame : ${}^c\underline{\mathbf{m}}^s \;=\; {}^\sharp\underset{\sim}{\mathbf{Q}}\; {}^\sharp\underline{\mathbf{m}}^s \qquad {}^c\underline{\mathbf{z}}^s \;=\; {}^\sharp\underset{\sim}{\mathbf{Q}}\; {}^\sharp\underline{\mathbf{z}}^s$.

This formulation of crystal plasticity using two local objective frames can be compared with Mandel's model [11], which involves a multiplicative decomposition of the deformation gradient. In fact rotation ${}^c\underset{\sim}{\mathbf{Q}}$ can be eliminated in the previous equations, and one can prove the model then is equivalent to Mandel's theory when elastic strains remain small [6]. The role played by the corotational frame in crystal plasticity becomes clear when one considers the simple shear test. If shear occurs in the plane of normal $\underline{\mathbf{n}} = (010)$ and in direction $\underline{\mathbf{d}} = [100]$, the stress oscillates as shown in figure 1 and we find that ${}^\sharp\underset{\sim}{\mathbf{Q}} = \underset{\sim}{\mathbf{1}}$ during the whole test. It means that the crystal directions follow the corotational frame. Because of the endless rotation of the corotational frame for simple shear, slip systems are successively activated and desactivated (figure 1). The result holds also for Mandel's theory (see also [1,3]), although the corotational frame does not explicitely appear in the model. The fact that the corotational frame displays an endless rotation for simple shear does not imply that the crystal orientation cannot stabilize. For $\underline{\mathbf{d}} = [\bar{1}10]$ and $\underline{\mathbf{n}} = (11\bar{2})$ for instance, the corotational and the lattice frames rotate in phase opposition so that ${}^c\underset{\sim}{\mathbf{Q}}\; {}^\sharp\underset{\sim}{\mathbf{Q}} = \underset{\sim}{\mathbf{1}}$.

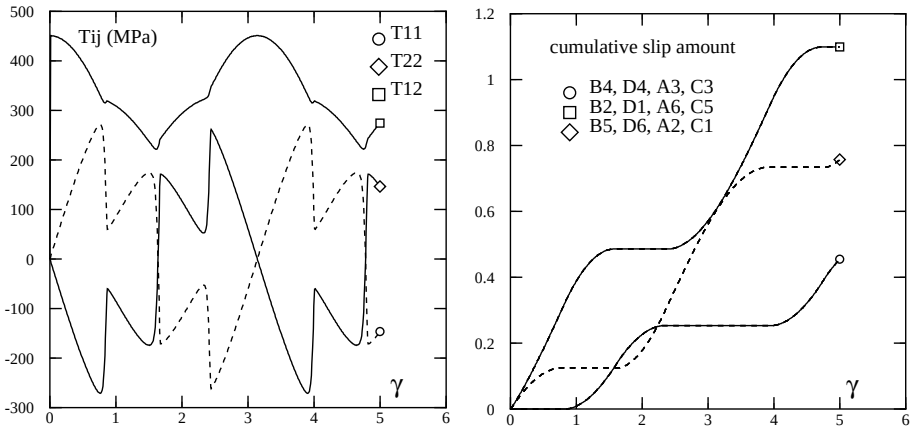

Figure 1 : Cauchy stress components and cumulative amounts of slip on slip systems during simple shear ($\underset{\sim}{\mathbf{F}} = \underset{\sim}{\mathbf{1}} + \gamma\,\underline{\mathbf{e}}_1 \otimes \underline{\mathbf{e}}_2$, single crystal with $\mu = 76190$ MPa, $\nu = 0.33$, $k = 150$ MPa $\mathrm{s}^{1/n}$, $n = 10$, $\tau_0 = 150$ MPa, mo hardening).

3. Finite deformation of polycrystals

The same method can be used to extend the models accounting for the elastoviscoplastic behaviour of polycrystals proposed in [4], to the finite strain framework. We restrict ourselves to isotropic elasticity. The additive strain rate decomposition (2) is still assumed. The overall viscoplastic strain rate is taken as the averaged viscoplastic strain

rate over all crystal orientations G

$$\underset{\sim}{\dot{\mathbf{e}}}^{p} \;=\; \sum_{g\in G} f^{g}\; \underset{\sim}{\dot{\mathbf{e}}}^{pg}, \tag{6}$$

where f^g is the volume fraction of orientation g. Interphase accommodation variables $\underset{\sim}{\beta}^g$, attached to the corotational frame (and therefore invariant), are introduced with the evolution rule

$$\underset{\sim}{\dot{\beta}} \;=\; \underset{\sim}{\dot{\mathbf{e}}}^{pg} \;-\; D\;(\underset{\sim}{\beta}^{g} \;-\; \delta\;\underset{\sim}{\mathbf{e}}^{pg})\sqrt{\tfrac{2}{3}\underset{\sim}{\dot{\mathbf{e}}}^{pg} : \underset{\sim}{\dot{\mathbf{e}}}^{pg}}. \tag{7}$$

We assume that an estimation of the mean stress over all grains having the same orientation can be explicitely computed knowing the stress $\underset{\sim}{\mathbf{S}}$ in the corotational frame, according to a concentration rule of the form:

$$\underset{\sim}{\mathbf{S}}^{g} \;=\; \underset{\sim}{\mathbf{S}} \;+\alpha\mu(\underset{\sim}{\mathbf{B}} \;-\; \underset{\sim}{\beta}^{g}), \tag{8}$$

where $\underset{\sim}{\mathbf{B}} \;=\; \sum_{g\in G}\; f^{g}\; \underset{\sim}{\beta}^{g}$. At small strain, the combination $(\alpha = 1, D = 0)$ corresponds to a Kröner-based model [8], whereas the so-called static model is obtained for $\alpha = 0$. An appropriate choice of D, δ and $\alpha = 1$, leads to a concentration rule which is numerically identical to Berveiller and Zaoui's one [2] corresponding to the self-consistent scheme. The constitutive behaviour of the individual grains is the same as in the previous section (viscoplastic formulation):

$$\underset{\sim}{\dot{\mathbf{e}}}^{pg} \;=\; \sum_{s\in S} \dot{\gamma}^{sg}\;\{\,{}^{c}\underline{\mathbf{m}}^{sg} \otimes {}^{c}\underline{\mathbf{z}}^{sg}\}, \qquad \dot{\gamma}^{sg} = (\max(0, F^{sg})/k)^{n}\;\mathrm{sign}\;\tau^{sg}, \tag{9}$$

$$F^{sg} = \mid \tau^{sg} \mid \; -(\tau_0 + q\sum_{r\in S}\; h_{sr}\; v^{rg}), \quad \text{with} \quad \dot{v}^{sg} = \mid \dot{\gamma}^{sg} \mid, \tag{10}$$

where $\tau^{sg} = \underset{\sim}{\mathbf{S}}^{g} : ({}^{c}\underline{\mathbf{m}}^{sg} \otimes {}^{c}\underline{\mathbf{n}}^{sg})$ is the resolved shear stress on slip system s in grain g. The rotation of the lattice frame associated with each orientation still follows evolution rule (5), where subscripts g must be added.

A fully self-consistent scheme for elastoplastic polycrystals at finite strain has been proposed in [10]. The behaviour of each grain is described by Mandel's model. However no explicit concentration rule can be worked out, and an intricate integral equation must be solved at each step. In contrast the method proposed here is a more pragmatic approach which advantageously combines micromechanical and phenomenological aspects, with a view to structural calculations using the finite element method.

4. Texture evolution

For the evaluation of a polycrystal model, attention should be paid to both the overall stress-strain response and texture evolution. The predicted textures can be compared with the results given by more classical models (Taylor-based, static models...), for given grain hardening properties, or for a given macroscopic stress-strain response. In the first case, the resulting overall responses will be very different, and in the second case, the material parameters must be modified for each model so as to obtain overall stresses of the same magnitude. In this work, the comparison has been made for both cases. In figure 2, the texture evolution is shown for a tensile test. The initial texture is isotropic, and is represented by 1000 random orientations in the numerical simulation. The material parameters are $\{\mu = 30$ GPa$, \nu = 0.33,\ \alpha = 1,\ D = 60,\ \delta = 0.01,\ \tau_0 = 140$ MPa$,\ q = 120$ MPa$,\ h_{ii} = 1$ (no summation) $,\ h_{ij} = 3$ (i $\neq$ j)$\}$, and approximately correspond to aluminium (k and n are chosen to get an almost rate-independent response). Figure 3 shows textures obtained after rolling, that can be compared with classical experimental data.

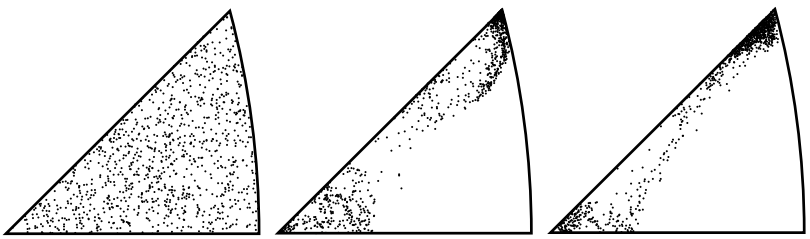

Figure 2 : Initial isotropic texture (left) and final texture after tensile straining using the proposed model (middle) and a Kröner-type model (right), (64%, logarithmic strain, inverse pole figure, 1000 orientations).

However the previous tests do not induce any rotation of the corotational frame. That is why we have then considered a simple shear test on an anisotropic aluminium sheet. The initial and the final texture after shearing in the plane 1-2 and in direction 1, are given in figure 4. One observes a global rotation of the quasi-orthotropic initial texture and some distorsion.

Finally it must be noted that, for a given macroscopic response, the final texture also depends on the form of the interaction matrix h_{ij} (diagonal, isotropic or with strong latent hardening as in the previous case). Furthermore more realistic stress-strain responses after large straining require the use of local non-linear hardening contrary to the previous illustrative cases.

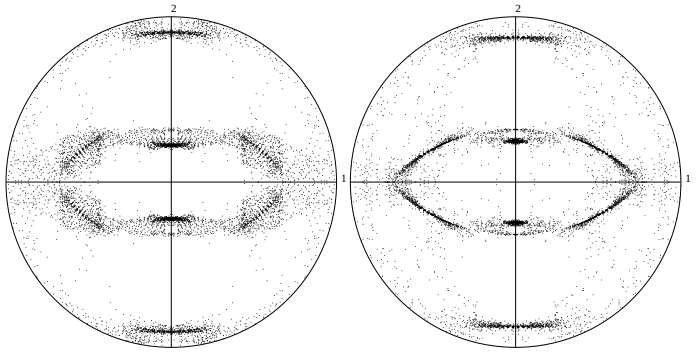

Figure 3 : $< 111 >$ rolling texture with the proposed model (left, $\delta = 0.1$, $q = 100$ MPa) and a Kröner-based model (right) (-128%, logarithmic strain, direct pole figure, 2016 orientations).

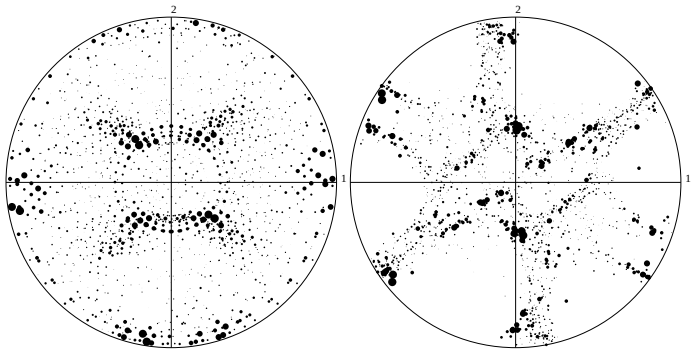

Figure 4 : Anisotropic initial texture and final texture after simple shear ($\underset{\sim}{\mathbf{F}} = \underset{\sim}{\mathbf{1}} + \gamma \underline{\mathbf{e}}_1 \otimes \underline{\mathbf{e}}_2$, $\gamma = 1$, 423 orientations).

5. References

1 Bertram, A., Kraska, M. : Beschreibung finiter plastischer Deformationen von Einkristallen mittels materieller Isomorphismen, ZAMM **75** (1995), 179-189.

2 Berveiller, M., Zaoui, A.: An extension of the self-consistent scheme to plastically-flowing polycrystals, J. Mech. Phys. Solids **20** (1979), 325-344.

3 Boukadia, J., Sidoroff, F. : Simple shear and torsion of a perfectly plastic single crystal in finite transformations, Arch. Mech. **40** (1988), 497-513.

4 Cailletaud, G. : A micromechanical approach to inelastic behavior, Int. J. Plasticity **8** (1992), 55-73.

5 Dogui, A., Sidoroff, F. : Rhéologie anisotrope en grandes déformations, in Rhéologie des matériaux anisotropes, CR 19e col. GFR Paris, Cepadues, Toulouse (1986).

6 Forest, S., Pilvin, P. : Large deformation of solids with microstructure, internal report ENSMP (1994).

7 Gilormini, P., Rougée, P. : Taux de rotation des directions matérielles dans un milieu déformable, C.R. Acad. Sci. Paris **t. 318** Série II (1994), 421-427.

8 Kröner, E. : Zur plastischen Verformung des Vielkristalls, Acta Metall. **9** (1961), 155-161.

9 Ladevèze, P. : Sur la théorie de la plasticité en grandes déformations, internal report LMT No. 9 (1980).

10 Lipinski, P., Krier, J., Berveiller, M. : Elasto-plasticité des métaux en grandes déformations: comportement global et évolution de la structure interne, Rev. Phys. Appl. **25** (1990), 361-388.

11 Mandel, J. : Equations constitutives et directeurs dans les milieux plastiques et viscoplastiques, Int. J. Solids Structures **9** (1973), 725-740.

12 ROUGÉE, P. : A new Lagrangian intrinsic approach to large deformations in contiuous media, Eur. J. Mech. A/Solids (1991), 15-39.

Addresses: DR. SAMUEL FOREST, CNRS/Ecole Nationale Superieure des Mines de Paris UMR 7633, B.P. 87 91003 Evry, France, Samuel.Forest@mat.ensmp.fr; PROF. DR. PHILIPPE PILVIN, Ecole Centrale de Paris, MSSMAT, Grde voie des Vignes 92295 Châtenay-Malabry, France, pilvin@mssmat.ecp.fr.